We are IntechOpen, the world's leading publisher of Open Access books Built by scientists, for scientists

6,900
Open access books available

186,000
International authors and editors

200M
Downloads

154
Countries delivered to

Our authors are among the

TOP 1%
most cited scientists

12.2%
Contributors from top 500 universities

CLARIVATE ANALYTICS
BOOK CITATION INDEX
INDEXED

WEB OF SCIENCE™

Selection of our books indexed in the Book Citation Index
in Web of Science™ Core Collection (BKCI)

Interested in publishing with us?
Contact book.department@intechopen.com

Numbers displayed above are based on latest data collected.
For more information visit www.intechopen.com

DFT Investigations on the CVD Growth of Graphene

Meicheng Li, Yingfeng Li and
Joseph Michel Mbengue

Additional information is available at the end of the chapter

Abstract

The chemical vapor deposition technique is the most popular for preparing high-quality graphene. Surface energy will dominate the nucleation process of graphene; thus, the surface energy problems involved in thin film growth are introduced first. The experimental tools to describe the growth process in detail are insufficient. So, a mass of simulation investigations, which can give out a very fine description of the surface atomic process, have been carried out on this topic. We mainly summarized the density functional theory works in unearthing the graphene nuclei process and mechanisms. In addition, some studies using molecular dynamics methods are also listed. Such a summary will be helpful to stimulate future experimental efforts on graphene synthesis.

Keywords: Surface energy, graphene, density functional theory, chemical vapor deposition

1. Introduction

After the graphene has been prepared perfectly on a nickel surface by the chemical vapor deposition (CVD) method, [1] the 2D crystal formation process on a perfect cleavage plane suddenly becomes a very important issue that needs to be deeply understood and penetrated. Similar to the general surface absorption phenomenon, the basic physical laws under graphene's formation on a metal surface should be the minimization of surface energy. What's special is that the classic surface energy theory, to some extent, seems to be slightly "broad-

brush." To explain and describe the perfect morphology of the obtained graphene crystals on a metal surface, we need to provide a very fine description of the process of graphene growth on a metal surface using CVD technology. This description should contain two main aspects:

1. The real-time surface energy variations from the absorption of a single carbon atom on the metal surface, to the nucleation of graphene, to the formation of a large-scale single-layer graphene, and finally to the formation of multilayers of graphene

2. The stationary state on-surface atomic structures and morphologies of the carbon phase on the metal surface, as well as the surface energies of the different surface carbon morphologies.

The main results are listed in Table 1. The aim of this chapter is to introduce the specific surface energy problems in the formation of 2D crystal graphene on metal surfaces, which are helpful for materials selection and process optimization in the fabrication of 2D carbons and other materials.

Classification	Method	Brief descriptions
Stationary state researches	DFT	Investigated the decomposition of CH_4 on Cu, and declared the active species should mainly be CH_x for graphene growth [2]
	DFT	Identified a carbon atom approaching induced bridging-metal structure formation on Cu [3]
	DFT	C atoms should be unstable on Cu surface but diffuse directly to the subsurface [4]
	DFT	Chain configuration is superior and will dominate the Ni surface until the number of C reaches 12 [5]
	DFT	Linear C chain owns 6 atoms should be the representative structure on copper surface [6]
	DFT	With increased concentration, C atoms will undergo a sinking and up-floating process on Cu surface [7]
	DFT	Graphene nucleation is very likely to start from the stepped regions, but can easily grow over the step [8]
	DFT	Revealed an energetic preference for the formation of stable 1D carbon nanoarches consisting of 3–13 atoms when compared to 2D compact islands of equal sizes [9]
Real-time kinetic researches	Exp.	Analyzed the activation energy paths for graphene nucleation and growth on Cu [10]
	Theo.	Paved the way for graphene growth on Cu based on Langmuir adsorption and 2D crystallization theory [11]
	Exp.	Using carbon isotope labeling, clearly verified that graphene growth on Ni occurs by a C dissolving–precipitating process whereas it grows by a surface adsorption process on Cu [12]
	MD	On Ni surface, high C concentration leads to the formation of graphene island and at ~1000 K, the graphene quality can be significantly improved [13]

Classification	Method	Brief descriptions
	MC	Showed the morphological evolution process of graphene growth on Pt surface [14]

DFT, density functional theory; MD, molecular dynamics; MC, Monte Carlo; Exp., experimental characterization; Theo., theoretical analysis.

Table 1. Summarization of researches on the surface process of graphene growth

By the present experimental technologies, it is still a great challenge to obtain the abovementioned knowledge especially under high-temperature conditions. So, it naturally becomes the best choice to investigate the graphene on-surface growth process by the accurate, reliable theoretical approach: the density functional theory (DFT). [15] Except for some controllable numerical approximations, the DFT approach can be recognized as a rigorous accurate theory, and since it is based on the maximum advanced of physical theory today, the results obtained by the DFT approach is of great reliability. Using the DFT approach, the graphene on-surface growth process can be described even at the level of electron distribution. In recent years, DFT researches on this aspect have been in full swing and some key progresses have been obtained, e.g., the surface energy evolution curve with the carbon atom number increases during the graphene growth on cupper surface has been revealed in detail by Li et al. [6] Parts of these theoretical results have been verified in experiments, and thus can provide reliable guides to optimize the preparation of graphene.

In this chapter, the surface energy problems involved in thin film growth will be first introduced from the aspect of the classic surface energy theory. Then, we will introduce the approaches that have been exploited in describing the graphene CVD growth process from the energy aspect using the DFT approach. Thirdly, we will review the achievements using these approaches on the growth process of graphene.

2. Surface energy problems in thin film growth

2.1. General fundamentals of surface energy

Consider the atoms in the bulk and surface regions of a crystal, the atoms in the bulk possess lower energy since they are more tightly bound, while the ones on the surface will possess higher energy since they are less tightly bound. The sum of all the excess energies of the surface atoms is the surface energy. Therefore, surface energy is generally defined as the excess energy needed when a new surface is created. [16]

For a liquid, the surface energy density is identical to the surface tension (force per unit length), e.g., water has a surface energy density of 0.072 J/m^2 and a surface tension of 0.072 N/m (the units are equivalent). For a solid, if we cut a body into pieces, it will consume energy. Under the hypothesis that the cutting process is reversible, according to the conservation of energy, the energy consumed by the cutting process will be equal to the energy inherent in the two

new surfaces created. Therefore, the unit surface energy of a solid material would be half of its energy of cohesion. In practice, this is only an approximate description. Surfaces often change their form away from the simple "cleaved bond" model implied above, and readily rearrange or react to reduce their energy.

Surface energy is the essence of "energy." According to statistical thermodynamics, the surface energy can be described by the Gibbs isotherm. [17] From the expression of Gibbs free energy in differential form, $dG \equiv -SdT + VdP + \gamma dA$, it can be defined as $\gamma \equiv \left(\frac{\partial G}{\partial A}\right)_{T,P}$. Therefore, surface energy can be considered as a criterion at equilibrium. When a system is reaching the equilibrium state, it tends to reduce its free energy. In some cases, this stable state is achieved by the reduction of the surface energy. This principle of surface energy determines many physical phenomena. For example, the smaller drops will aggregate into larger ones; in the absence of gravity, a droplet will tend to become spherical to reduce its surface energy.

Most importantly, the relative magnitude of surface energy determines the wettability of one material on another material. A material having very low surface energy can easily wet a material having high surface energy and form a uniform adhesive layer on it. Conversely, if the deposition material has a higher surface energy, it readily forms an atomic group on the substrate with lower surface energy. Such a function of the surface energy has a wide range of practical applications. We can coat surface-modified materials (e.g., pigments) on the surface of buildings, automobiles or mechanical components to modify their surface energy and thus adapt to the working environment. A good example is waterproofing. Since organic material has low surface energy, coating wax on the surface of a vehicle can prevent the formation of water film when the automobile is wet with rain. Another important application, which is mainly discussed in this chapter (i.e., wettability), is that it determines the process of thin film growth and the quality of the samples obtained. This will be discussed in detail in Section 1.1.3.

2.2. Determination of the surface energy

To measure the surface energy of a liquid, commonly, there are two methods. The first one is the so-called stretching film method, as illustrated in Figure 1. By this method, the surface energy is measured by stretching a liquid membrane (which increases the surface area and hence the surface energy density). In that case, in order to increase the surface area of a mass of liquid by an amount, $2\delta L$ (the liquid membrane has two surfaces), a quantity of work, $F\delta$, is needed. The increase of the surface energy is $2\gamma\delta L$ (where γ is the surface energy density of the liquid). So, $2\gamma\delta L = F\delta$, the surface energy density can be calculated by $\gamma = F/2L$.

The other commonly used method to measure the surface energy of a liquid is the capillary tube method, as illustrated in Figure 2. When inserting a capillary tube of greater surface energy into the liquid, the adhesive force of the liquid to the tube wall will point upward. Thus, to reduce the amount of energy, the liquid will rise along the tube till a new equilibrium is reached: $f\cos\theta = mg$. f is the adhesive force, which is equal to $2\pi R\gamma$ (R is the radius of the capillary, γ is the surface energy density of the liquid). θ is the contact angle between the liquid and the capillary. mg is the gravity of the liquid column, which equals to $\pi R^2 h\rho g$ (h is the height of rise in the capillary and ρ is the density of the liquid). Therefore, the equality can be rewritten
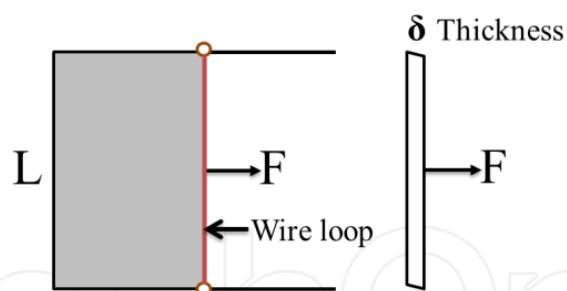
Figure 1. A liquid membrane stretched by an external force.

as $2\pi R\gamma\cos\theta = \pi R^2 h\rho g$, then the surface energy of the liquid can be calculated by $\gamma = R\rho gh / 2\cos\theta$.
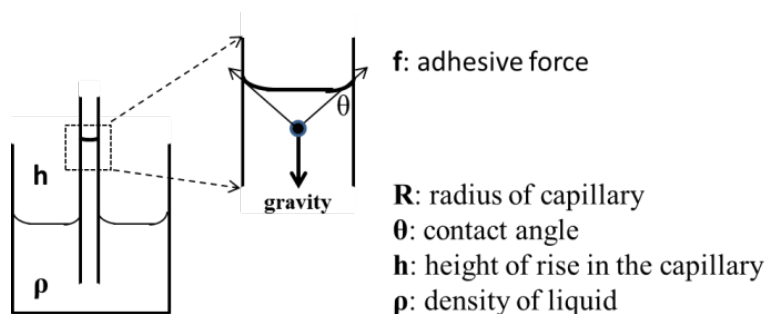

Figure 2. Illustrations for the capillary tube method in measuring the surface energy of a liquid.

For the measurement of the surface energy of a solid, the above two methods cannot be used. But there exists one way which is approximate to the capillary tube method in the case of liquids. This is called the zero creep method. At some high temperatures, the solid creeps and even though the surface area changes, the volume remains approximately constant. If over-hanging a cylindrical line of radius r and length l, at equilibrium, the variation of the total energy vanishes and we have

$$\mathrm{d}E = 1/2\rho g\pi\left(2l^2 r\mathrm{d}r + 2r^2 l\mathrm{d}l\right) - 2\pi\gamma\left(r\mathrm{d}l + l\mathrm{d}r\right) = 0$$

where ρ is the density, and γ is the surface energy density of the solid line. Since the volume of the solid line remains constant, the variation of the volume is zero, i.e.

$$\pi r^2 l = \pi\left(r + \mathrm{d}r\right)^2\left(l - \mathrm{d}l\right)$$

From these two equations, the expression of the surface energy for a solid can be deduced as $\gamma = r\rho gl/2$, which is similar as that of the liquid deduced from the capillary tube method. So,

the surface energy density of the solid can be obtained by measuring the radius and length of a cylindrical line, at equilibrium.

This method is only valid for isotropic solids, whose surface energy is the same in all orientations. Such a condition can be strictly satisfied only for amorphous solids. If the sample is a metal or made by powder sintering (like ceramics), isotropy is also a good approximation. In the case of single-crystal materials, which are obviously anisotropic, this method will become invalid. In addition, since the measurement conditions for the surface energy of a solid requires high temperature, the obtained results sometimes will be inaccurate and thus unreliable in practical applications. So, in determining the surface energy of a solid, theoretical methods are of special importance. The traditional theoretical methods in estimating the surface energy of a solid include the thermodynamics calculation and mechanical calculation methods.

In the thermodynamics calculation method, the surface energy of a solid at a given temperature is derived by the thermodynamic relations from the measured value under a melting state. So, the calculated surface energy is also only valid for isotropic solids. In the mechanical calculation method, the surface energy of a solid is related to its Young's modulus. But since the Young's modulus for many materials is nearly the same, the obtained values are quite coarse with about six to seven multiples of errors. Additionally, both the thermodynamics and mechanical calculation methods can't reflect the relationships between the surface energy and the crystallographic orientations. So, they are mostly used for some particular systems or in cases that require less precision.

The third theoretical method is called the atomic calculation method. In this method, the surface energy is determined by multiplying the energy of one bond and the number of bonds being broken. According to the different approaches in obtaining the energy of one bond, this method can be split into two branches. In the first one, the energy of one bond is estimated by the sublimation energy. For the crystal owning one mole (N_A) atoms, at least $0.5 N_A$ bonds will be formed. In consideration of the coordination number Z, the number of bonds in one-mole crystal will be $0.5 N_A*Z$. So, the average energy per bond can be estimated as $\varepsilon = \frac{\Delta H_s}{0.5 N_A * Z}$. ΔH_s is the molar enthalpy of sublimation. In the other one, the energy of one bond is calculated by the interatomic potential, which can be calculated using the modern molecular simulation method or the first principle method. Take the FCC crystal as an example, the coordination number of every atom is 12. While the atoms at the (111) plane only possess nine coordination atoms. This means that 3 bonds per atoms are broken during the formation of a (111) plane in the FCC crystal. So, the energy required to form one surface atom can be given as: $E(111) = \varepsilon*3 \equiv \frac{\Delta H_s}{2 N_A}$. The surface energy γ can be defined as $\gamma \equiv E(111) \times$ number of surface atom / surface area. For the (111) plane in FCC crystal, the number of surface atom / surface area equals $\frac{4}{\sqrt{3}a_0^2}$. So, $\gamma = \frac{\Delta H_s}{2 N_A}\left(\frac{4}{\sqrt{3}a_0^2}\right) = \frac{\Delta H_s}{\sqrt{3}N_A a_0^2}$.

2.3. Thermokinetics process in thin film growth

During the thin film growth process, an old surface will be covered and a new surface will be created. Thus, this process should be mainly controlled by the surface energy theory. Therefore, the growth thermokinetics as well as the quality of the obtained samples will be controlled by the surface energy. In the first, the critical size of the surface nucleation in thin film growth

and the nucleation rate are determined by the surface energy. In this section, the thermodynamic process of thin film growth on the flat surface is illustrated to introduce this determination relationship.

In order to study step generation on a flat surface, we consider the case of forming a disc with radius r and height a (an atomic layer), as illustrated in Figure 3. We assume that the material of the disc is the same as the flat surface and the disc is grown epitaxially, the additional surface energy caused by the formation of the disc is only the surface energy on the side region of the disc,

$$E_d = 2\pi ra\gamma$$

This increased surface energy will exert a compressive force on the disc,
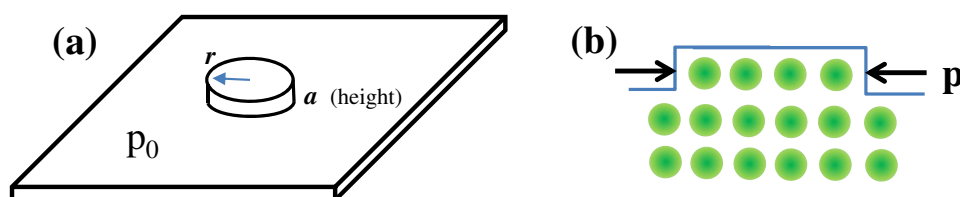
Figure 3. (a) The disc nucleation on flat surface with height a and radius r; (b) schematic cross-sectional view of the disc (the side of the disc exerts a compressive force on it).

$$p = \frac{1}{A}\frac{dE_d}{dr} = \frac{2\pi a\gamma}{2\pi ra} = \frac{\gamma}{r}$$

where A is the surrounding area of the disc. Under such a compressive force, the energy of each atom in the disc will increase

$$p\Omega = \frac{\gamma\Omega}{r}$$

where Ω is the atomic volume. Due to the energy increase, the atoms in the disc become much easier to sublimate than those in the flat substrate. The sublimation rate can be written as

$$J_c' = N_0\upsilon_s \exp\left(-\frac{\Delta G_{des}}{kT} + \frac{\gamma\Omega}{rkT}\right) = J_0 \times \exp\left(\frac{\gamma\Omega}{rkT}\right)$$

where N_0 is the number of atoms being absorbed on the flat surface per unit area, υ_s is the RMS velocity of atoms on the flat surface, ΔG_{des} is the activation energy during the desorption

process of the surface atom. At a given temperature, J_c' and J_0 are both proportional to the pressure, so the pressure ratio on the disc and the flat surface is

$$\frac{p}{p_0} = \exp\left(\frac{\gamma\Omega}{rkT}\right)$$

From this equation, the energy changes per atom from the gas phase to the solid phase can be calculated as $\Delta\mu = kT\ln(\frac{p}{p_0})$, thus the sublimation heat per unit volume ΔE_s can be calculated by $\Delta E_s = \frac{\Delta\mu}{\Omega}$.

Consider the energy change from the gas phase to the solid phase during the disc growth, including the surface energy being increased and the sublimation heat being released,

$$\Delta E = E_s - V\Delta E_s = 2\pi ra\gamma - \pi r^2 a\Delta E_s = 2\pi ra\gamma - \pi r^2 a\frac{\Delta\mu}{\Omega}$$

From this equation, the critical size (here means the critical radius r_c) of the surface nucleation can be defined. Let $\frac{d\Delta E}{dr} = 0$, we can obtain

$$r_c = \frac{\gamma\Omega}{\Delta\mu}$$

If the radius of the disc reaches r_c, the energy change ΔE_c will equal

$$\Delta E_c = \pi r_c a\gamma$$

This energy is defined as the nucleation activation energy, which determines the nucleation rate

$$\text{nucleation rate} \propto \exp\left(-\frac{\Delta E_c}{kT}\right) = \exp\left(-\frac{\pi a\gamma^2\Omega}{kT\Delta\mu}\right)$$

In the second, the growth mode of thin film means that the layered growth or island growth is also controlled by the surface energy. Such control is illustrated in the heteroepitaxial growth of a thin film on a flat substrate, taking the (001) facet growth of simple cubic crystal as an example, and only the nearest-neighbor interactions are considered. Let thin film of material A grow on surface B, the interaction potential between two A atoms and two B atoms is

indicated by U_{AA} and U_{BB}, respectively, and the interaction potential between atoms A and B is indicated by U_{AB}. According to the definition of the surface energy, the surface energies of material A and B, and the interface energy between material A and B can be calculated as

$$\gamma_A = u_{AA} / 2a^2$$
$$\gamma_B = u_{BB} / 2a^2$$
$$\gamma_{AB} = \left[\frac{u_{AA}}{2a^2} + \frac{u_{BB}}{2a^2} - \frac{u_{AB}}{a^2} \right]$$

where a is the lattice constant (the same for A and B). If $u_{AB} \geq u_{AA}$, which means $\gamma_B \geq \gamma_A + \gamma_{AB}$ (the film growth will reduce the energy of the system), the material A will wet the surface of material B completely, which results in a layered thin film growth process. If $u_{AB} < u_{AA}$, which means $\gamma_B < \gamma_A + \gamma_{AB}$ (the film growth will increase the energy of the system), material A can't completely wet material B, which results in an island thin film growth process.

In the initial stage of the thin film growth, there are only very few atoms. The concept of surface energy, which is a collection quantity for a given material, seems too big to be used in analyzing the growth process. So, in practice, for fine studies on the thin film nucleation process, energy evolution on the atomic and even on the electric level based on the theoretical method (specially the molecular simulation technology) is always used.

3. Approaches from energy aspect in investigating graphene growth

Graphene is the first truly 2D crystal ever observed in nature,[18] as shown in Figure 4. This is remarkable because 2D crystals were predicated to be unstable and thus inexistent in the past, due to the Mermin–Wagner theorem. This theorem states that a 2D crystal will melt at any temperature but zero due to thermal fluctuations. From its discovery, graphene has grabbed appreciable attention due to its exceptional electronic and optoelectronic properties: it is reported as one of the best electronic materials. The reported properties and applications of graphene have opened up new opportunities for future devices and systems.
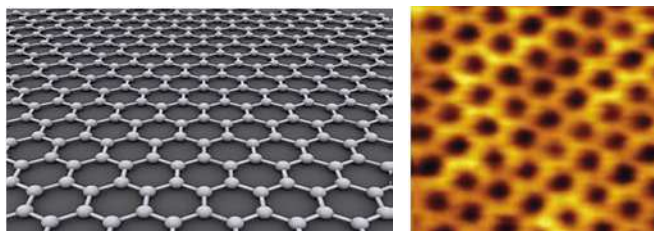

Figure 4. Illustration and the scanning probe microscopy image of graphene. (Haider I. Rasool, Emil B. Song, Matthew Mecklenburg, et al., JACS, 2011)

Because of the great application potential of graphene, investigations on the synthesis of single sheets of graphene have also attracted a large number of researchers and companies. Till now, the synthesis routes of graphene can be broadly categorized into five main different sections[19]: the exfoliation and cleavage route, the chemical vapor deposition techniques, thermal decomposition of SiC or other substrates, unzipping CNTs, and chemical methods. Among them, the chemical vapor deposition technique is the most popular for preparing large-scale and high-quality graphene samples. Most of the chemical vapor deposition growth of graphene uses nickel, iron, and copper foils as the substrate. While nickel and iron have great carbon solubility, the graphene growth will go through a carbon dissolving and precipitating process. [12] Therefore, on nickel and iron foils, the obtained graphene films are often inhomogeneous with many defects and multilayer flakes. Such disadvantage can be overcome by using copper foil as the substrate due to its low carbon solubility. The growth process of graphene on copper foil is self-limited, thus large-scale high-quality single-layer samples can be obtained. So, here, we focus on the formation of graphene on copper substrate. To investigate the nucleation and growth mechanism of graphene on copper surface systematically is of great importance for exploiting and optimizing the fabrication of graphene by the chemical vapor deposition technique.
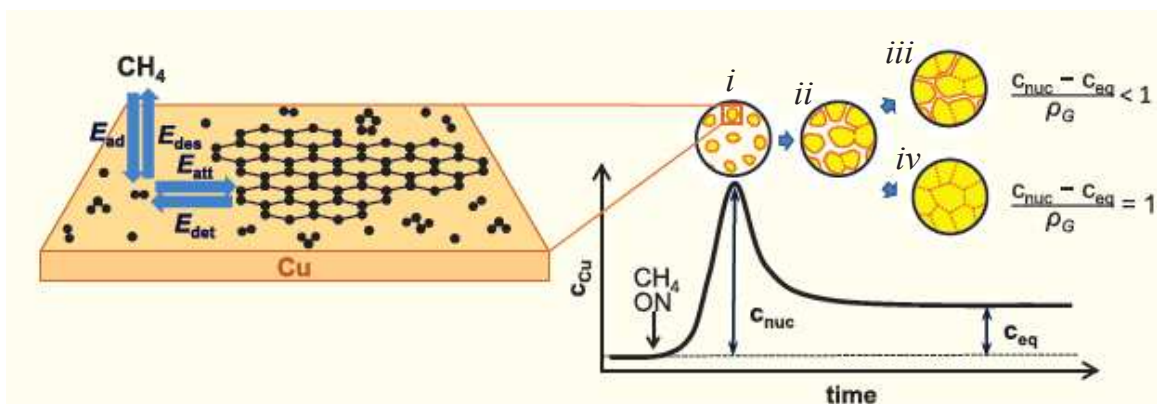

Figure 5. Growth mechanism of graphene on Cu surface. Methane is adsorbed on the surface and then decomposed to carbon adatoms. When the supersaturation of the carbon adatoms reaches a critical value (C_{nuc}), graphene begins to nucleate and grow step by step.

Through experimental method, by characterizing the graphene nuclei grown on copper for different growth temperatures and times by high-resolution scanning electron microscope, Kim et al. [10] have analyzed the nucleation and growth mechanism of graphene on copper substrates (as shown in Figure 5). Methane molecules are first chemisorbed on the copper surface. Such adsorbed methane can be decomposed to carbon adatoms. The concentration of these carbon adatoms, C_{cu}, increases with time increases, until a critical point, i.e., the supersaturation of the carbon adatoms reaches a critical value (C_{nuc}). Now, graphene begins to nucleate. Such process and the growth of the nuclei will deplete the carbon surrounding them. So, C_{cu} decreases quickly. In this decreasing process, the nucleation rate becomes negligible, while the growth of formed nuclei continues. Till the C_{cu} is reduced to a stable level, C_{eq}, the equilibrium between graphene, surface carbon, and CH_4/H_2 will be reached.

Analyses based on the experimental characterizations can give the framework of graphene growth similar to the existing theories for two-dimensional nucleation and growth of thin films. However, encumbered by the growth conditions of graphene and the lack of effective characterization methods, some fine messages, like the exact nature of the active carbon species adsorbed on the Cu surface, the adsorption and desorption energy of the carbon species on the Cu surface, the surface diffusion energy barrier, as well as the bonding process of the carbon species, cannot be well obtained yet. These messages are of great importance. The first-principle method, especially the density functional theory (DFT), is much suited for the investigation of such messages. By this method, a lot of simulation studies have been carried out on the atomic process of graphene growth on copper substrates.

DFT is a computational quantum mechanical modelling method, which is among the most popular and versatile methods available in physics, chemistry, and materials science. With this method, the properties of the system are determined by using functionals, i.e., functions of another function, which in this case is the spatially dependent electron density. DFT has broad applications in the chemical and material sciences for the interpretation and prediction of complex system behaviors. Specifically, DFT computational methods are applied for the study of systems exhibiting high sensitivity to synthesis and processing parameters. In this section, we will briefly introduce the primary approaches that have been exploited in investigating the growth mechanisms of graphene on copper surface.

3.1. The approaches that have been exploited in investigating graphene growth

As mentioned above, the system tends to reduce its free energy as it reaches the equilibrium state. So, the most direct approach in investigating the growth process of graphene is the so-called geometry optimization approach, to study the geometry configuration evolution of the system with carbon atoms on copper surfaces by minimizing free energy. By DFT technology, during such evolution processes, the bond breaking and formation can be presented virtually, and the optimized configuration close to the real nucleation form can be obtained. For example, through carrying out configuration evolution calculations on the system containing 4–6 carbon atoms on the copper(111) surface, Li et al. [6] found that, at the very first stage, linear chains will be formed and dominate the copper surface, as illustrated in Figure 6.
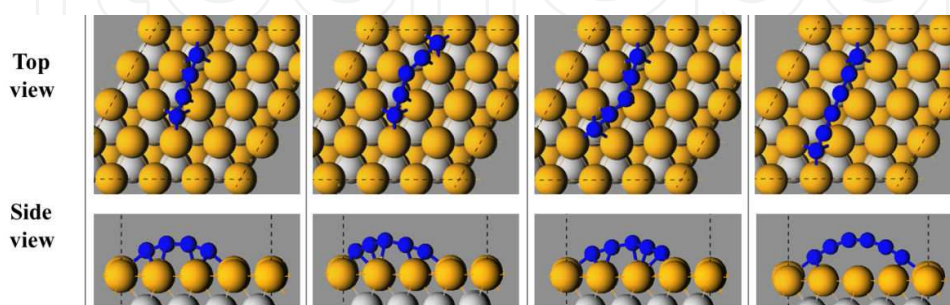

Figure 6. Top and side views for the stable configuration of system containing 4–6 carbon atoms on copper(111) surface.

It is easy to imagine that, if several carbon atoms are absorbed on the copper surface, there will be some different nucleation forms, e.g., four carbon atoms will have four different forms as illustrated in Figure 7. These four configurations are obtained by geometry optimizations starting from different initial configurations with carbon atoms arranged on different locations. Depending on the laws of statistical thermodynamics, the occurrence probabilities of these different configurations will be dramatically determined by their configuration energy. So, calculating and comparing the stable energies of different possible configuration is also the commonly used approach in investigating the graphene growth process.
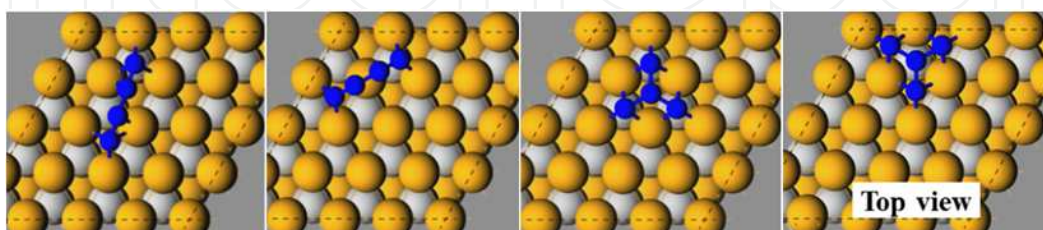
Figure 7. Different nucleation forms of four carbon atoms on Cu(111) surface.

The growth process of graphene is a dynamic chemical reaction process, thus it is not only determined by the energies of the reactants (initial configurations) and products (stable configurations), but also deeply influenced by the activation energy. The transition state search technology in DFT method can offer these messages quite well. For example, Wu et al. [3] have used the climbing image nudged elastic band method to search the transition state of a 1 + 1 (the bonding of two carbon atoms on Cu(111) surface) reaction, and identified the minimum energy path (MEP) of this reaction, as shown in Figure 8. First, the carbon atom remaining on the surface (carbon B) rotates around the bridging Cu to its neighboring site (Figure 8c), with a 0.51 eV barrier. Then, it rotates further toward carbon A with an activation energy of 0.64 eV. Finally, by conquering a 0.37 eV barrier, carbon B drags carbon A to the surface and forms a dimer (Figure 8e). This MEP with several barriers thus gives a very rugged part of the two-adatom potential energy surface.

To reveal the realistic nucleation process of graphene on copper surface, the quantum mechanics/molecular mechanics (QM/MM) method should be more suitable than the above approaches since it can consider the real reaction temperature and model the growth kinetics and nonequilibrium processes. However, since it contains quantum mechanics calculations, the computational efficiency is very low and thus this method can't handle large systems and can't model long enough times to reproduce the real reaction process. So, till now, few reports [2] using such approaches have been found.

The next best approach in revealing the dynamics nucleation process of graphene is the molecular dynamics (MD) method, based on empirical atomic force field. The MD method can simulate the real physical movements of every atom in a system of interacting atoms. The movement trajectories of every atom are determined by solving Newton's equations of motion numerically, where the interatom forces are defined by interatomic potentials (atomic force field). The precision and reliability of the MD method is much lower than the DFT method
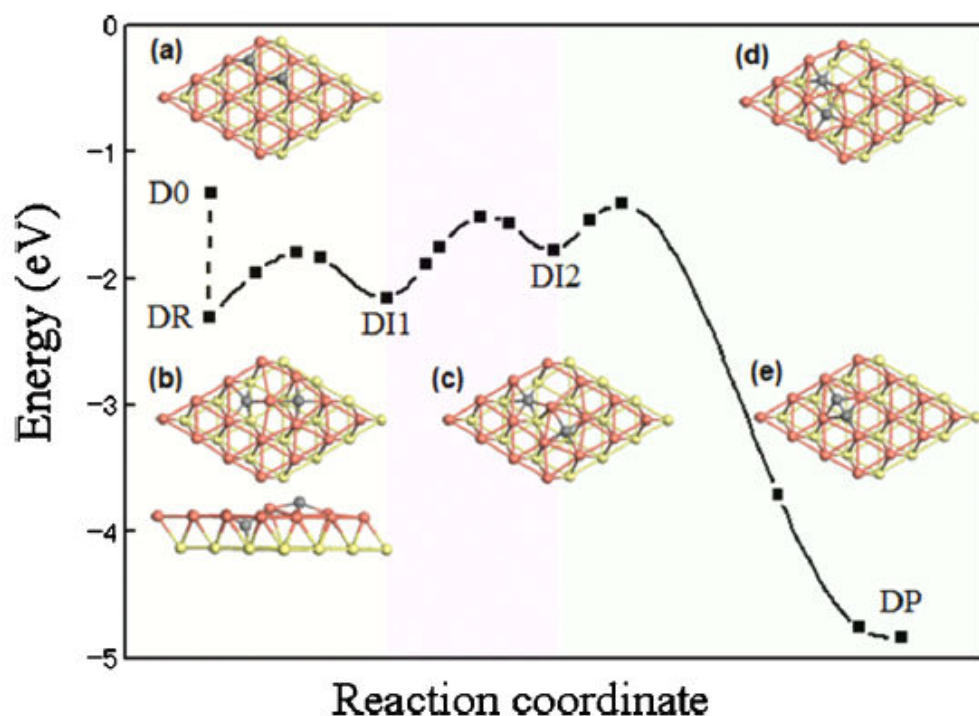
Figure 8. Minimum energy path of the 1 + 1 carbon atom reaction on copper(111) surface.

since they dramatically depend on the force field, which is fixed and thus cannot take the chemical conditions of atoms into account. While, just because of the coarse graining of the MD method compared with the DFT method, it can deal with systems consisting of a vast number (tens of thousands) of atoms. Using MD simulation based on the ReaxFF force-field, Ding et al. [13] have found that after 100 ps MD simulation at 1000 K, high C concentration leads to the formation of graphene islands, as shown in Figure 9.
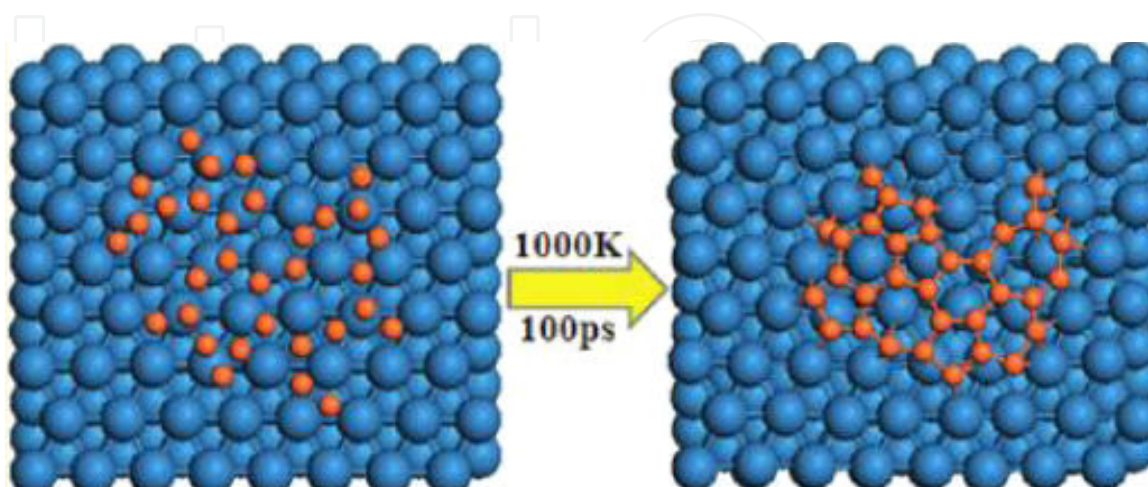
Figure 9. Initial and final structures obtained in 100 ps MD simulations at 1000 K for 32 carbon atoms.

In summary, upon investigating the nucleation behaviors of carbon atoms to form graphene, four main approaches have been exploited. These approaches can provide intuitive images in the nucleation process of graphene, and some very useful messages in analyzing the surface reaction path. Besides these four approaches, the Monte Carlo simulation method[14, 20] has been also used. Since the Monte Carlo method provides similar messages as the DFT method with less accuracy, we did not discuss it here.

4. Achievements on investigations of graphene growth

4.1. The exact nature of the active carbon species in graphene growth

Hydrocarbon decomposition is the first step in the growth of graphene on copper surface, which determines the exact nature of the active carbon species. By the DFT calculations, Zhang et al. [2] investigated the decomposition process of CH_4 on a five-layer $p(3 \times 3)$ copper slab by the transition state search technology. The initial state is an adsorbed CH_4 molecule, and the final product is a C atom plus four H atoms on the surface. There are three intermediates, namely, methyl (CH_3), methylene (CH_2), and methylidyne (CH). As shown in Figure 10, all four dehydrogenation steps are endothermic, and the corresponding activation energy barriers are about 1.0–2.0 eV. The final product C + 4H is already 3.60 eV higher in energy than the adsorbed CH_4, which suggests that atomic carbon is energetically very unfavorable on Cu surface. According to their results, the active species for graphene growth on the copper surface should not be carbon atoms but mainly CHx (especially CH). This is quite different from the case of other active metal surfaces, such as Pd, Ru (where the decomposition of CH_4 is exothermic), and Ni (decomposition of CH_4 is slightly endothermic).

Zhang's work is quite helpful to understand the growth mechanisms of graphene at the very initial stage. While, in spite of these insights, in most DFT investigations on the nucleation of graphene, atomic carbons are used. Surely, one of the main reasons for using atomic carbons is for simplicity (the situations will become very complicated if CHx is used as the active species). Besides, the more reasonable reason for using atomic carbons as the active species in graphene growth is that it is still hard to determine certain active carbon species for graphene growth on copper surface: since there exist complex surface morphologies on real copper substrates in experiments, the active site for the dehydrogenation of CHx might not be located at the plane copper surface but perhaps near the step regions, which should introduce significant influences on the dehydrogenation energy. In addition, to grow graphene on copper surfaces, dehydrogenation should finally be completed. To determine the exact nature of the active carbon species in graphene growth, further investigations are quite necessary.

4.2. The stable configuration of 1-2 carbon atoms on the copper surface

By experimental methods, the growth mechanism of graphene on copper substrate has been demonstrated to be a surface adsorption process. So, naturally, the carbon atoms should be more stable on the surface than in the bulk of the copper lattice. However, by comparing the absorption energy of carbon atoms on different locations in the 4 × 6 copper(111) slab, as shown
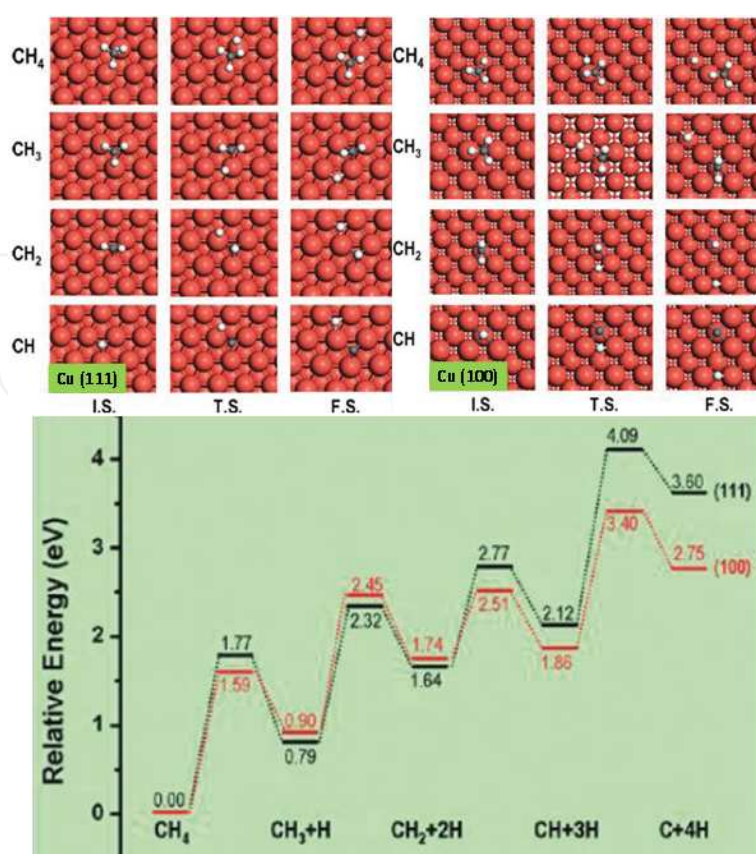
Figure 10. Geometric structures of the initial state (I.S.), transition state (T.S.), and final state (F.S.) of the four steps of CH$_4$ dehydrogenation on Cu(111) and Cu(100) surface (top); their energy profile is also shown (bottom).

in Figure 11, Riikonen et al. [4] found that the HCP adsorption site is unstable. The FCC and BRI are also metastable sites; at finite temperatures, carbon diffuses directly to the subsurface A site. According to their analysis, the stabilization of carbon interstitials in the copper subsurface area can be understood with a few simple arguments. They state that, the copper atoms at the topmost layer are easily pushed toward the vacuum due to their low coordination numbers. Such greater flexibility of the topmost copper atoms compared with the bulk ones opens a gate to the carbon atoms, which can thus sink into the subsurface and form octahedrally symmetric copper surroundings.

The occurrence of sinking carbon atoms on the copper subsurface has been also found in the work of Wu et al. [3] through transition state searches for two next nearest neighboring carbon atoms to form a dimer on the surface (Figure 8). In their report, an almost linear C-Cu-C configuration (Figure 8b) was formed. They named it the bridging-metal (BM) structure. Through geometry optimization for the system having two carbon atoms on the Cu(111) surface, Li et al. [7] also found this so-called BM structure, as shown in Figure 12.

In conclusion, despite the growth mechanism of graphene on copper substrate being a surface adsorption process, the carbon atoms still have a chance to penetrate into the subsurface (solve in copper), especially under very low carbon atom concentrations. This means that under special process conditions, carbon atoms can also be implanted into the copper foil. Thus,
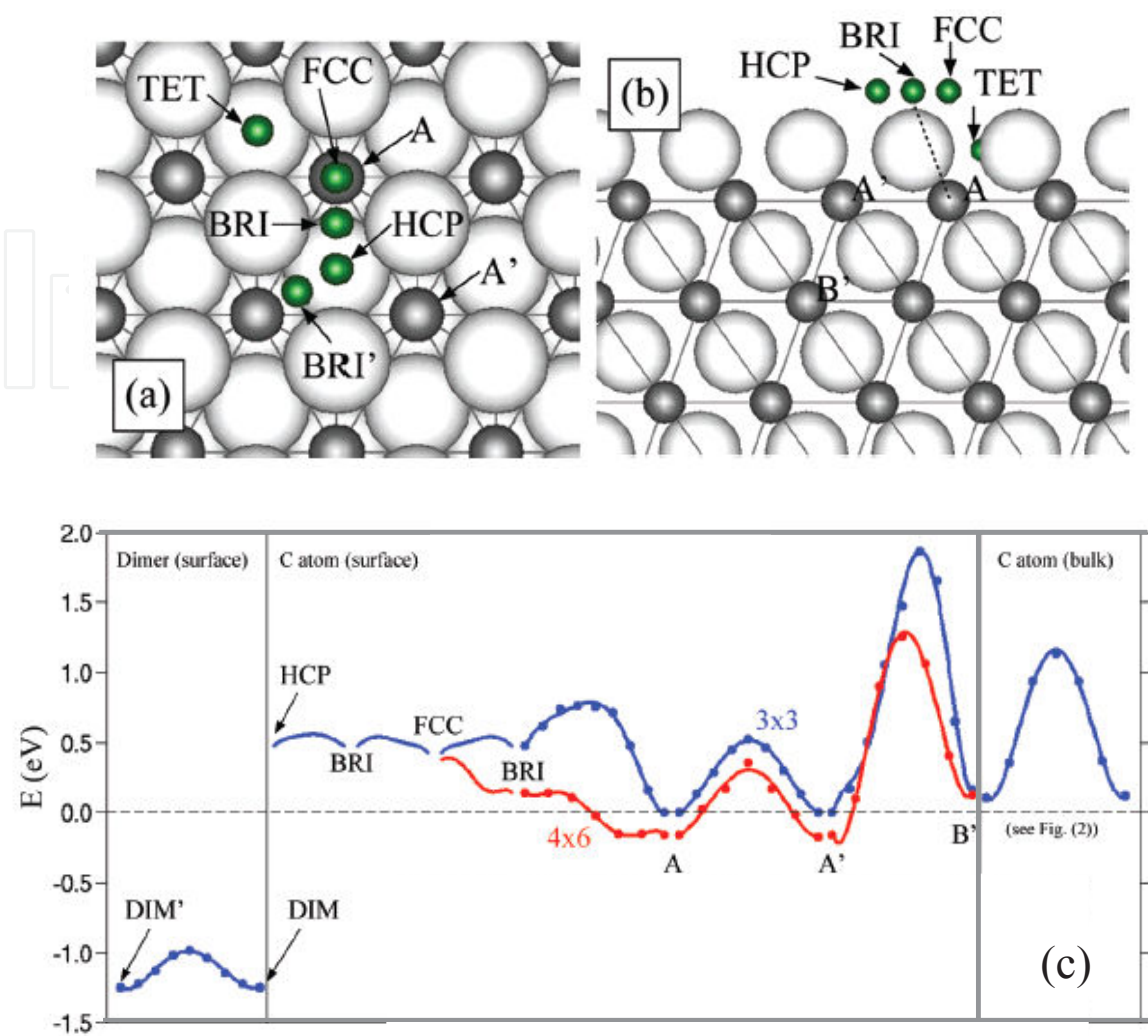
Figure 11. The Cu(111) surface, top (a) and side (b) views; carbon energetics and minimum energy paths on the Cu(111) surface, subsurface and in the bulk (c). The small green and dark spheres denote the surface and octahedral adsorption sites, respectively. Surface adsorption sites contain four inequivalent styles: FCC, HCP, TET, and BRI. BRI′ is a neighboring equivalent site to BRI.

graphene can be formed by following high-temperature annealing, which results in the migration of implanted atoms to the surface and eventually bonding to each other. Such a technique has successfully been used.

In the usual fabrication process of graphene by CVD technology, such a "sinking" of carbon atoms into the copper subsurface will have nearly no influence on the surface adsorption growth of graphene, firstly because dimer formation and the subsequent graphene growth is by far the most favorable reaction in both energetic and kinetic terms. [12]. Secondly, Li et al. [7] have investigated the following behavior of the sunken carbon when more carbon atoms are absorbed around it. They found that, the sunken carbon atom will spontaneously form a dimer with one of the newly adsorbed carbon atoms, and the formed dimer will up-float on the top of the surface again, as shown in Figure 13.
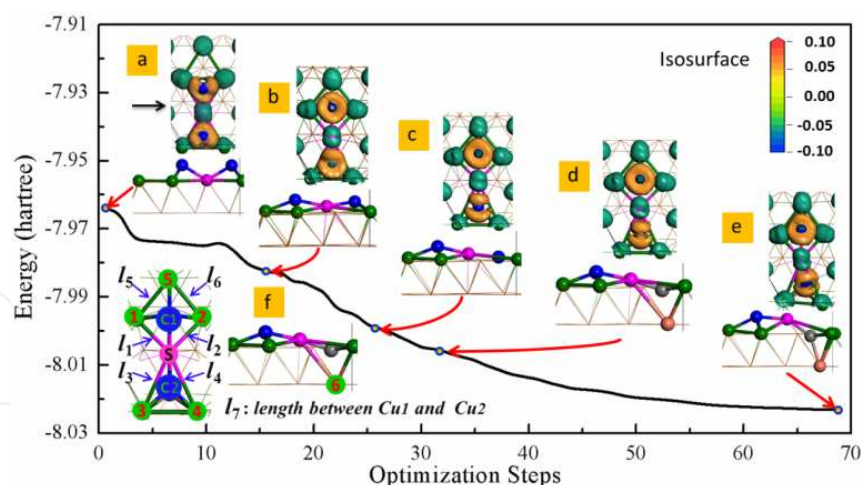
Figure 12. Geometry optimization paths from two on-surface carbon atoms to the BM structure. The deformation electrodensities are mapped to characterize the bonding situations.
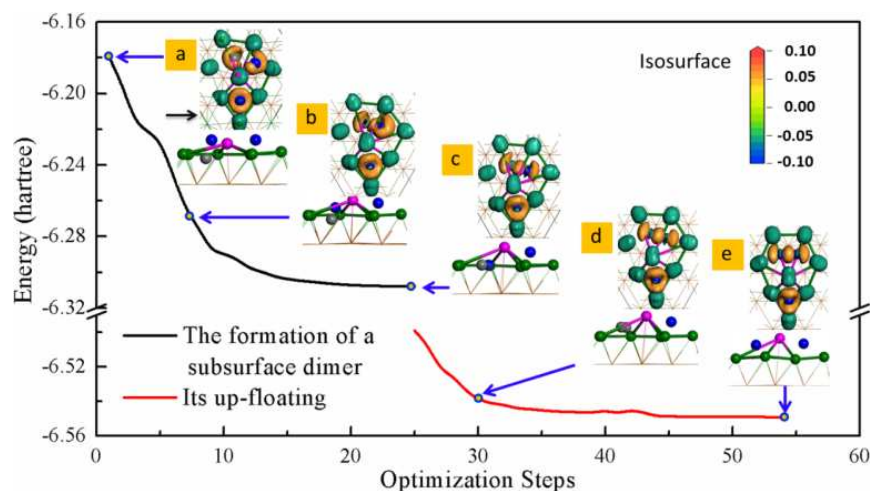

Figure 13. Geometry optimization paths for the system with one carbon atom absorbed near the BM structure.

4.3. Configuration selectivity of the initial carbon clusters

Through DFT calculations, Gao et al. [5] have investigated the stable configurations of carbon clusters containing 1 to 24 atoms on the Ni(111) surface. For different configurations of the carbon clusters with the same size, they analyzed their stability by comparing the absorption energies (so-called formation energy), as given in Figure 14. They found that, within the entire size range of their calculations, carbon chains on the Ni(111) surface are always more stable than ring configurations of the same size. The crossover between the carbon chains and the C-sp2 network occurs at $N = 12$, beyond which the energy difference between chain and sp2 configurations becomes larger and larger. This means that, during the graphene growth on Ni(111) surface, until $N = 12$, the C chain configuration is superior and will dominate the metal surface. A ground state structural transition from a C chain to a C-sp2 network (graphene island) occurs at $N = 12$.
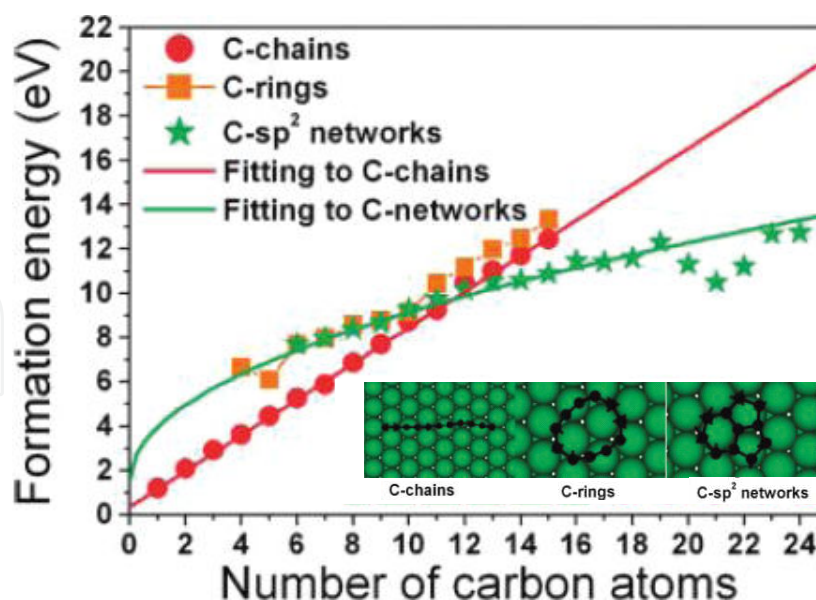
Figure 14. Formation energies of chains, rings, and most stable sp2 networks on the Ni(111) surface versus the number of carbon atoms.

For the case of copper surfaces, Li et al. [6] have investigated the graphene nucleation path by importing carbon atoms step by -step. At every step, they exhausted all possible configurations and discussed their stability. Based on careful configuration and energy analyses, an overall path of graphene nucleation has been proposed in Figure 15. At the very first stage, the linear chains containing 4 to 10 carbon atoms will be formed and dominate the copper surface, while both the Y-type and circular carbon species are energetically repelled. Then, the growth of the carbon cluster encounters an energy barrier at about 0.25 eV. By conquering such a barrier, the carbon clusters will present Y-type (furcate) structures. Then, by adsorbing new carbon atoms step by step, ring-containing carbon structures and graphene nuclei will be formed, with energetic preference. Their results suggest that, it will be difficult to form furcate and ring-containing carbon structures at the very initial stage of graphene nucleation, but it should be formed when the linear chains have grown to some length.

Based on analysis of the deformation electrodensity maps of the linear carbon chains containing 4 to 10 atoms (Figure 16), Li et al. [6] have also discussed the bonding situation between the linear chain and the copper surface. The green color in Figure 16 indicates that net electrons remain and stable chemical bonds are formed. Through bonding situation analyses, they point out L6 should be a representative structure. In the linear carbon chains, when the number of carbon atoms is less than 6, not only the end- but also the mid-carbon atoms bond stably with the copper surface; if the number of carbon atoms reaches 6, the mid-carbon atoms are completely detached from the copper surface, and thus an arc is formed.

4.4. Continuous growth of graphene over steps

In the chemical vapor deposition fabrication of graphene on copper surface, it has been found that the growth of macroscopic pristine graphene is not limited by the underlying copper
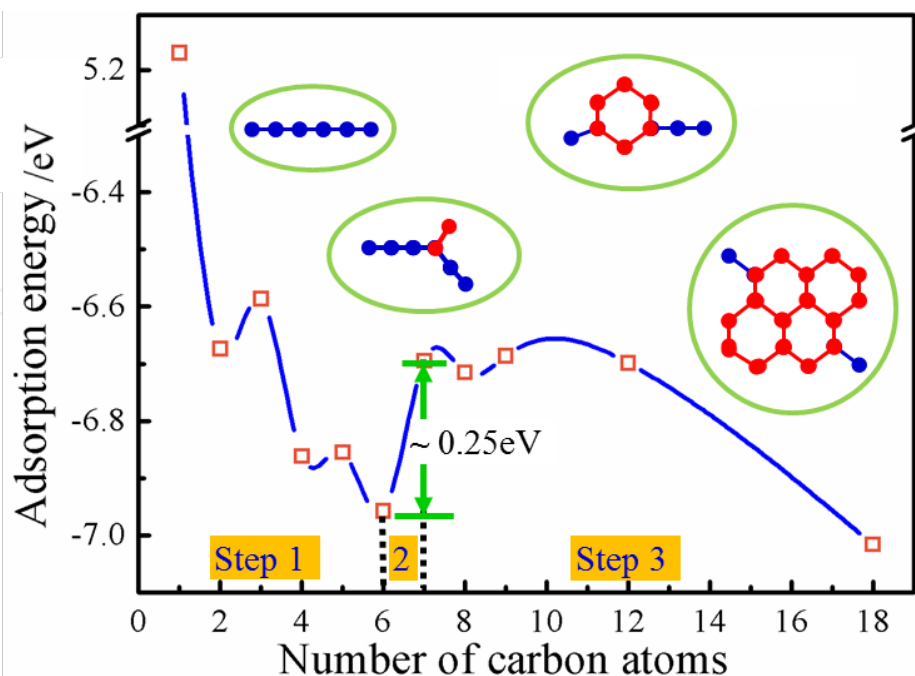
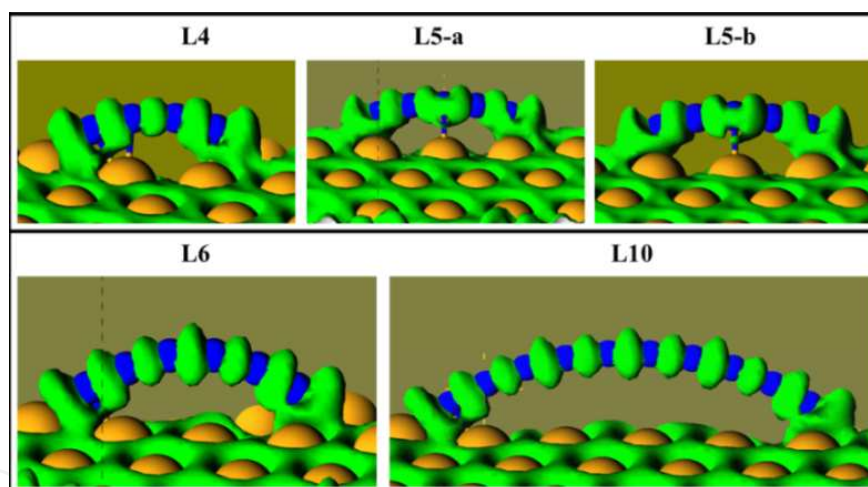**Figure 15.** Energy evolution curve of the overall nucleation path of graphene growth.

Figure 16. Deformation electrodensity maps for the linear carbon chains.

structure. Haider et al. [21, 22] have characterized the surface morphology of the copper substrate and the graphene grown by scanning tunneling microscopy (STM), as shown in Figure 17. They revealed that the atomic arrangement of graphene was not affected by the morphology and atomic arrangement of the copper substrate. This feature implies practical value for the mass production of high-quality graphene on rough copper substrates.

Inspired by this experimental phenomenon, Li et al. [8] have investigated the coalescence of carbon atoms over a copper monatomic step by the DFT calculations. They constructed a monatomic step as shown in Figure 18a, and carefully explored how the carbon atoms bond together over the step. Firstly, they put some carbon atoms on and under the steps separately.
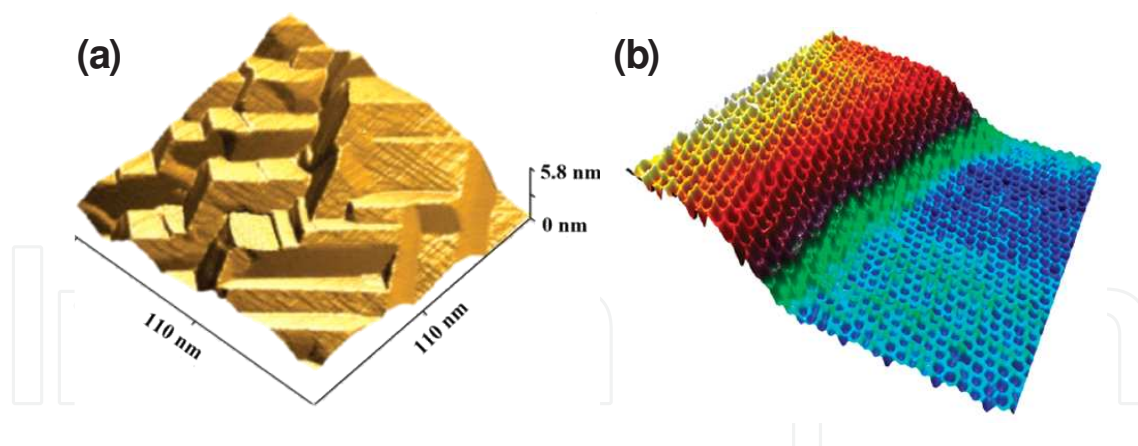
Figure 17. (a) STM topograph of a highly corrugated region of the sample. (b) Atomic resolution STM topograph over a copper monatomic step.

In some special cases, as shown in Figure 18b, after geometric optimizations, the separated carbon atoms can successfully bond together. Additionally, this over-step coalescence of the carbon atoms is spontaneous as the energy evolution curve descends monotonically throughout all the geometry optimization steps. They attributed this success to the energy barrier preventing the bonding of the two carbon atoms, which is reduced significantly, since the two copper atoms between them are both shared by three carbon atoms and thus have weak interactions with the two bonded carbon atoms. However, the dimer formed finally moves up to the upper terrace but is not located on the over-step position. In their following DFT calculations, by importing another carbon atom to the "left hole" of the atom being drawn up to the upper terrace, they found that this over-step coalescence process is unrepeatable (Figure 18c). As a conclusion, the direct over-step coalescence of the carbon atoms separated by the steps is very difficult, and thus should not be the main pattern of graphene's continuous growth over the steps.

By importing additional carbon atoms between the existing ones separated by the steps, they found that the main way in which graphene grows over the steps continuously is that the carbon atoms, adsorbed additionally on the locations between the already existing ones which are separated by the steps, link them (these carbon atoms separated by the steps) together. They first imported one additional carbon atom, as illustrated in Figure 19a. The obtained configurations after geometry optimization show a positive trend to a successful over-step coalescence of carbon atoms. Then, one more carbon atom is imported again in the optimized configurations as shown in Figure 19b. Finally, the new carbon atom links the separated ones together, and a cambered over-step carbon chain was formed.

During the calculations of the absorption energies, they found that the adsorption energy of the single carbon atom near the steps (5.91–6.48 eV) is about 1.0 eV higher than that adsorbed on a flat copper surface (5.13–5.17 eV). This indicates that carbon nucleation should be very likely to start from the stepped regions. The thermodynamic reason is that around the step regions on the substrate, the surface energy is higher than that on the flat regions.
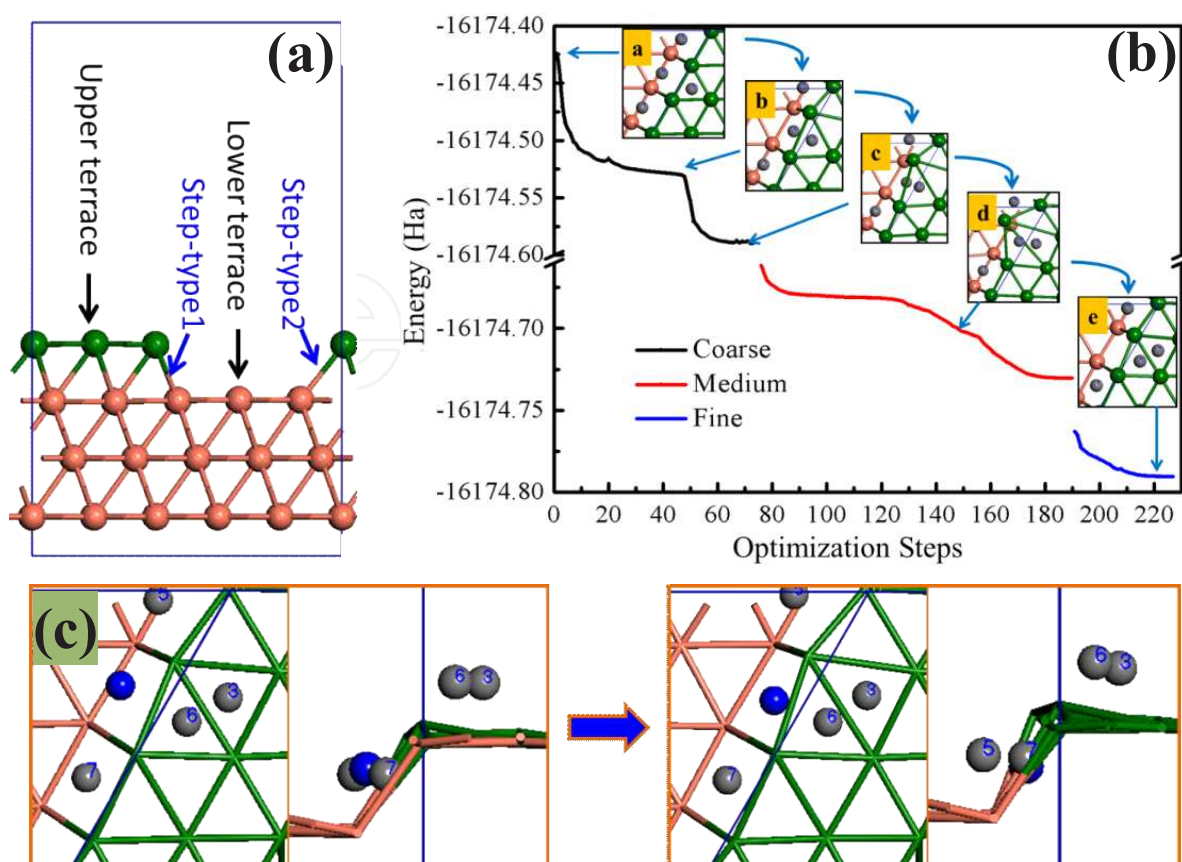
Figure 18. (a) Side view of Cu(111) surface separated on terraces by monatomic steps. (b) Energy evolution curves and corresponding key configurations during the direct over-step coalescence of the carbon atoms. (c) The direct over-step coalescence of the carbon atoms is unrepeatable.
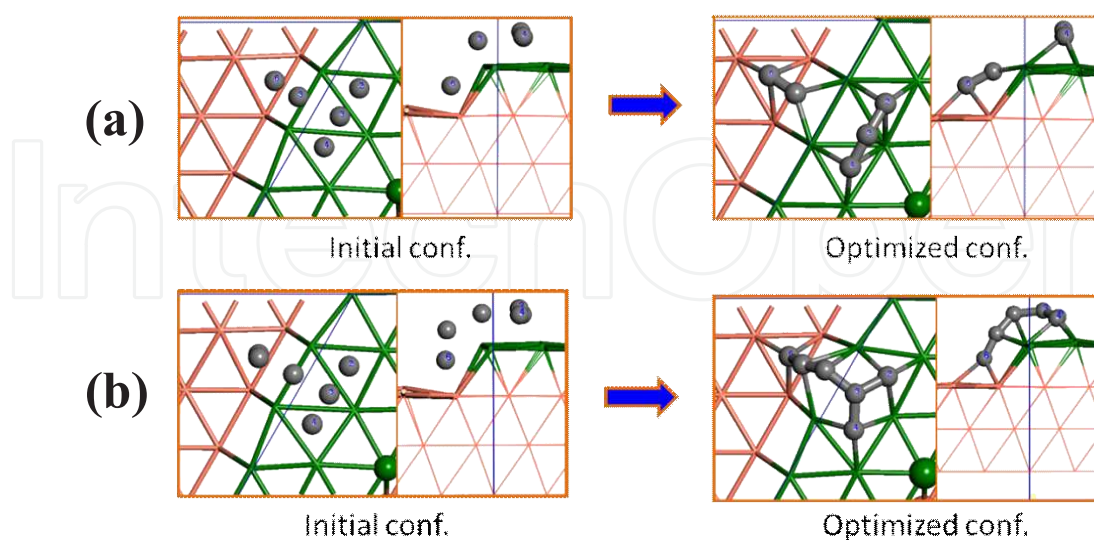

Figure 19. (a) Initial and optimized configurations after importing one additional carbon atoms on the step. (b) Those after importing the second additional carbon atoms on the step.

4.5. Molecular dynamics simulations on graphene growth

Since graphene's growth is typical of a kinetic and nonequilibrium process. Molecular dynamics is a powerful tool to explore such processes at the atomic level. Based on the reactive force-field (ReaxFF), Ding et al. [13] have investigated the evolution of carbon structures and the growth kinetics of graphene on Ni(111) surface. Taking into account that the carbon concentration is raised gradually during the chemical vapor deposition experiments on graphene growth, they firstly investigate the effect of carbon concentration on the nucleation of graphene, as illustrated in Figure 20. By arranging 16 and 32 carbon atoms on the Ni surface, namely, 1/8 and 1/4 monolayers, they found that at the low concentration (16 carbon atoms), the carbon monomers readily enter the subsurface, which is identical to the DFT results above. As the carbon concentration increases, after 100 ps annealing, nearly all of the carbon atoms, which are arranged coincidentally to contain long chains or large polygonal rings, eventually form a sp2 network of pentagons, hexagons, and heptagons. As a summary, low concentrations do not allow the formation of large sp2 network, and high concentrations are required to induce the formation of graphene islands.
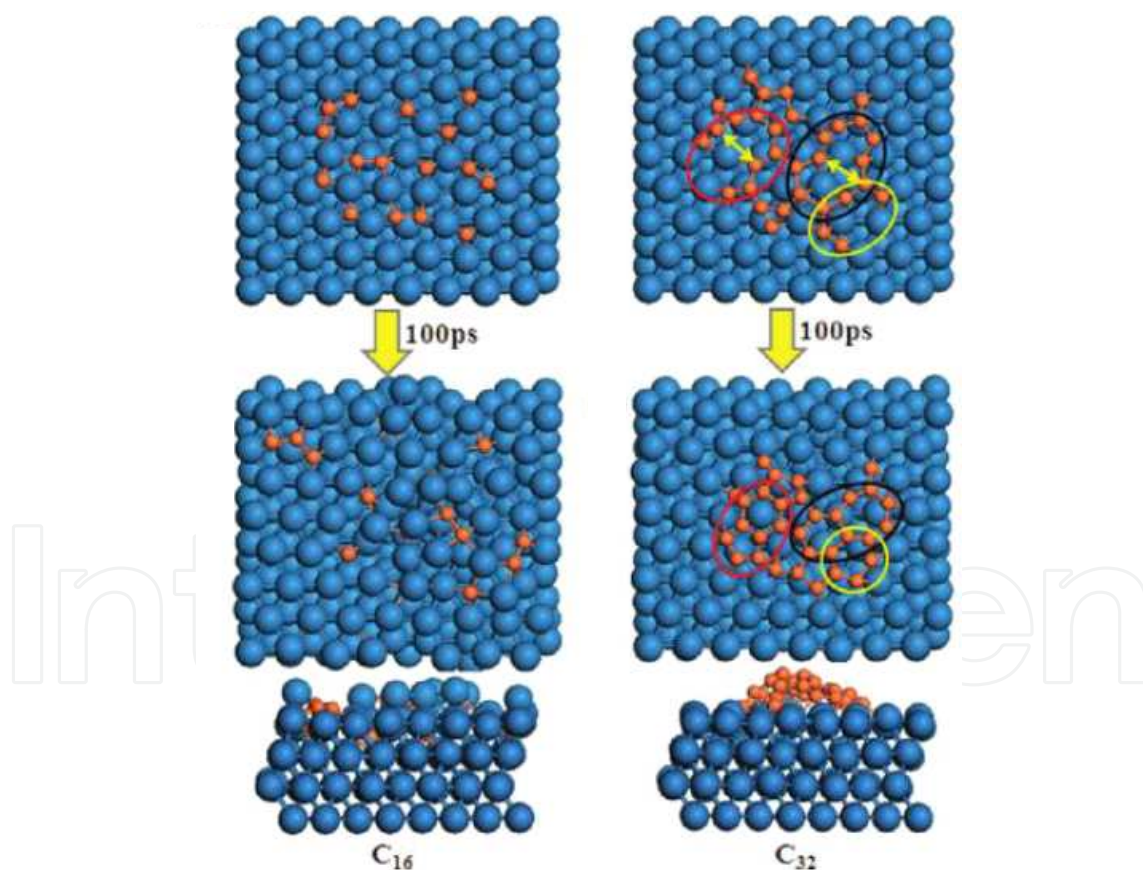

Figure 20. Initial and final structures obtained in 100 ps MD simulations at 1000 K for C16 and C32. Cyan and orange spheres represent Ni and C atoms, respectively.

Then, they turned to the influence of temperature on the formation of carbon structures. Under high carbon concentrations with 64 carbon atoms on the Ni surface, they analyzed the final

configuration (Figure 21) after 100 ps molecular dynamics simulation at four temperatures 800, 1000, 1200, and 1400 K. They summarized the number of i-membered rings (MRs) (i = 3, 4,…, 9) in the C structures formed at different temperatures in Table 2. With the increases in temperature, the fact that the number of 3- and 4-MRs are greatly reduced indicates that they are very unstable; the increased numbers of 5-MRs and 7-MRs show that they are very stable. The number of 6-MRs denotes the quality of graphene fabricated. According to their simulation, the number of 6-MR reaches the maximum at 1000 K and decreases as the temperature further increases. Their results indicate that the optimal growth temperature of graphene should be around 1000 K, as most CVD experiments of graphene growth were applied.
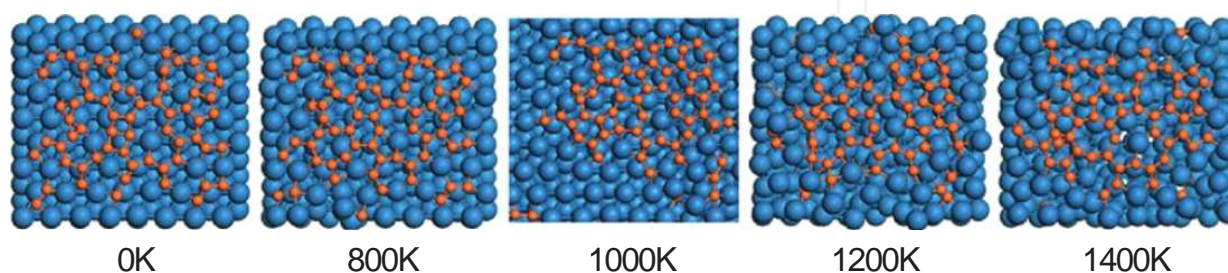

| 0K | 800K | 1000K | 1200K | 1400K |

Figure 21. Equilibrium configurations at 0, 800, 1000, 1200, and 1400 K.

T (K)	3-MR	4-MR	5-MR	6-MR	7-MR	8-MR	9-MR
0	6	3	1	2	1	0	1
800	1	0	2	3	2	1	1
1000	1	1	2	8	1	1	0
1200	1	0	2	5	1	0	0
1400	0	0	4	3	1	1	1

Table 2. Number of various polygons in the equilibrium configurations

Through simulating the growth of graphene islands by adding carbon atoms around it, they found that graphene islands can grow larger by capturing deposited C atoms and forming more hexagons on the edge with its self-healing capabilities during growth.

5. Summary

The fundamental theory of surface energy and the corresponding problems involved in thin film growth have been briefly introduced in this chapter. For the special issue of graphene growth on metal surface under the frame of chemical vapor deposition technology, the growth

process and the quality of samples obtained is also determined by the surface energy theory. But due to the high-temperature growth conditions of graphene and the lack of effective real-time characterization methods, the fine messages of key importance in analyzing the thermo-kinetics process of graphene growth are difficult to obtain by experimental measurements. Therefore, DFT investigations on the nucleation process of graphene under chemical vapor deposition growth have been carried out very prosperously. The key approaches being exploited in describing the graphene CVD growth process have been introduced. And some main achievements, on investigating the growth process of graphene, using the DFT method and the molecular dynamics method, have been reviewed. Till now, in spite of high-quality graphene samples being fabricated successfully using the chemical vapor deposition technology, to develop a wider range of applications, the preparation of graphene with special structures, like single crystal graphene sheets, graphene nanoflakes, graphene nanoribbons, graphene nanomesh, and graphene quantum dots, still needs further investigations on their growth mechanisms. We hope the above contents are helpful for the improvement in the fabrication and application of graphene.

Author details

Meicheng Li[*], Yingfeng Li and Joseph Michel Mbengue

*Address all correspondence to: mcli@ncepu.edu.cn

State Key Laboratory of Alternate Electrical Power System with Renewable Energy Sources, School of Renewable Energy, North China Electric Power University, Beijing, China

References

[1] K. S. Kim, Y. Zhao, H. Jang, S. Y. Lee, J. M. Kim, K. S. Kim, J. H. Ahn, P. Kim, J. Y. Choi, and B. H. Hong, Nature 457, 706 (2009).

[2] W. H. Zhang, P. Wu, Z. Y. Li, J. L. Yang, J Phys Chem C 115, 17782-17787 (2011).

[3] P. Wu, W. H. Zhang, Z. Y. Li, J. L. Yang, J. G. Hou, J Chem Phys 133 071101-1:4 (2010).

[4] S. Riikonen, A. Krasheninnikov, L. Halonen, R. Nieminen, J Phys Chem C 116, 5802–5809 (2012).

[5] J. F. Gao, Q. H. Yuan, H. Hu, J. J. Zhao, F. Ding, J Phys Chem C 115, 17695-17703 (2011).

[6] Y. Li, M. Li, T. Wang, F. Bai, Y.-X. Yu, Phys Chem Chem Phys 16, 5213-5220 (2014).

[7] Y. Li, M. Li, T. Gu, F. Bai, Y. Yu, M. Trevor, Y. Yu, Appl Surf Sci 284, 207-213 (2013).

[8]   Y. Li, M. Li, T. Gu, F. Bai, Y. Yu, T. Mwenya, Y. Yu, AIP Adv 3 052130 (2013).

[9]   R. G. Van Wesep, H. Chen, W. Zhu, and Z. Zhang, J Chem Phys 134, 171105 (2011).

[10]   H. Kim, C. Mattevi, M. R. Calvo, J. C. Oberg, L. Artiglia, S. Agnoli, C. F. Hirjibehedin, M. Chhowalla, E. Saiz, ACS Nano 6, 3614-3623 (2012).

[11]   HoKwon Kim, Eduardo Saiz, Manish Chhowalla, and Cecilia Mattevi, arXiv preprint arXiv:1302.0179 (2013).

[12]   X. S. Li, W. W. Cai, L. Colombo, and R. S. Ruoff, Nano Lett 9, 4268 (2009).

[13]   L. J. Meng, Q. Sun, J. L. Wang, F. Ding, J Phys Chem C 116 6097-6102 (2012).

[14]   J. Y. Guo, C. X. Xu, F. Y. Sheng, Z. L. Shi, J. Dai, Z. H. Li, and X. Hu, J Appl Phys 111, 044318 (2012).

[15]   Koch W, Holthausen M C, Holthausen M C. *A Chemist's Guide to Density Functional Theory*. Weinheim: Wiley-Vch, 2001.

[16]   J. W. Mayer, L. C. Feldman *Electronic Thin Film Science: for Electrical Engineers and Materials Scientists*. Prentice Hall, 1992.

[17]   D. P. Woodruff, D. A. King *The Chemical Physics of Solid Surfaces. 10. Surface Alloys and Alloy Surfaces*. Elsevier, 2002.

[18]   K. S. Novoselov, A. K. Geim, S. V. Morozov, D. Jiang, Y. Zhang, S. V. Dubonos, I. V. Grigorieva, A. A. Firsov, Science 306, 666-669 (2004).

[19]   W. Choi, I. Lahiri, R. Seelaboyina, Y. S. Kang, Crit Rev Solid State Mater Sci 35, 52–71 (2010).

[20]   F. Ming, A. Zangwill, J Phys D Appl Phys 45 154007:1-6 (2012).

[21]   H. I. Rasool, E. B. Song, M. Mecklenburg, B. C. Regan, K. L. Wang, B. H. Weiller, J. K. Gimzewski, J Am Chem Soc 133, 12536-12543 (2011).

[22]   H. I. Rasool, E. B. Song, M. J. Allen, J. K. Wassei, R. B. Kaner, K. L. Wang, B. H. Weiller, J. K. Gimzewski, Nano Lett 11, 251-256 (2011).